

# Unzipping of a double-stranded block copolymer DNA by a periodic force

Ramu Kumar Yadav\* and Rajeev Kapri†

Department of Physical Sciences, Indian Institute of Science Education and Research Mohali,  
Sector 81, Knowledge City, S. A. S. Nagar, Manauli PO 140306, India.

(Dated: 21 January 2021)

Using Monte Carlo simulations, we study the hysteresis in unzipping of a double stranded block copolymer DNA with  $-A_nB_n-$  repeat units. Here  $A$  and  $B$  represent two different types of base pairs having two- and three-bonds, respectively, and  $2n$  represents the number of such base pairs in a unit. The end of the DNA are subjected to a time-dependent periodic force with frequency ( $\omega$ ) and amplitude ( $g_0$ ) keeping the other end fixed. We find that the equilibrium force-temperature phase diagram for the static force is independent of the DNA sequence. For a periodic force case, the results are found to be dependent on the block copolymer DNA sequence and also on the base pair type on which the periodic force is acting. We observe hysteresis loops of various shapes and sizes and obtain the scaling of loop area both at low- and high-frequency regimes.

## I. INTRODUCTION

Single-molecule manipulation techniques, which are now used routinely to study individual molecule by applying mechanical forces in the pico-newton ranges, has greatly increased our understanding of molecular interactions in biological molecules [1]. The unzipping of a double stranded DNA (dsDNA) by an external force, exerted by different enzymes or molecular motors *in vivo*, has biological relevance in processes like DNA replication and RNA transcription [2]. The unzipping transition has been studied for over two decades, both theoretically [3–8] and experimentally [9–11], by applying an external pulling force on the strands of the DNA. The dsDNA unzips to two single strands abruptly when the force exceeds a critical value showing first order nature of the phase transition [3, 4, 6–8]. If biomolecules are subjected to a periodic forcing, they can unbind and rebind with a hysteresis in their force-distance isotherms. The study of hysteresis in unbinding and rebinding of biomolecules can provide useful information on the kinetics of conformational transformations, the potential energy landscape, controlling the folding pathway of a single molecule, and in force sensor studies[12–16].

In recent years, the behavior of a dsDNA under a periodic force has been studied using Langevin dynamics simulation of an off-lattice coarse-grained model for a short homo-polymer DNA chains [17–21] and Monte Carlo simulations on a relatively longer chains of directed self-avoiding walk (DSAW) model of a homo-polymer dsDNA on a lattice [22–24]. In both type of studies, a dynamical phase transition was found to exist, where the DNA can be taken from the zipped state to an unzipped state with an intermediate dynamic state. It was found that the area of the hysteresis loop,  $A_{loop}$ , which represents the energy dissipated in the system, depends on the frequency of the periodic force. At higher frequencies, it

decays with frequency as  $A_{loop} \sim 1/\omega$ , whereas at lower frequencies, it scales with the amplitude  $g_0$  and frequency  $\omega$  of the oscillating force as  $A_{loop} \sim g_0^\alpha \omega^\beta$ . The values of exponents  $\alpha$  and  $\beta$  are however found to be different in these studies.

In this paper, we consider a hetero-polymer DNA as a block copolymer DNA, in which the heterogeneity is considered in the form of repeated blocks,  $A_nB_n$  or  $B_nA_n$ , where  $2n$  is the block length,  $A$  and  $B$  are different types of base pairs with two- and three- hydrogen bonds, respectively. One end of this DNA sequence is subjected to a pulling force while the other end is kept anchored. We considered both the constant and the periodic pulling force cases. The unzipping of a block copolymer DNA by a constant pulling force is found to be a first-order phase transition. The equilibrium phase boundary separating the zipped and the unzipped phases does not depend on the DNA sequence and is found to follow the same exact expression, as obtained for the homo-polymer DNA case [6, 8, 22], but with a different effective base pair energy. The results for the unzipping of a block copolymer DNA subjected to a periodic force are however found to be sequence dependent. For sequences of higher block lengths, the results also depend on whether the periodic force is acting on  $A$  type or  $B$  type base-pairs.

The paper is organized as follows: In Sec. II we define our model and simulation details. We also define the quantities of interest we are studying in this paper. Section III is devoted for discussions on our results for both the static and the periodic pulling force cases. We finally summarize the results of this paper in Sec. IV.

## II. MODEL

We define hetero-polymer DNA as a block copolymer DNA of type  $(A_nB_n)_M$ , where  $A$  and  $B$  are two different types of base pairs,  $2n$  is the total number of base pairs in a block unit, also be called as block length, and  $M = N/2n$  represents the total number of blocks in the DNA of length  $N$ . We consider block lengths  $2n = 4, 8, 16, 32, 64, 128$  and  $256$ . The two strands of the

\* ramukumar@iisermohali.ac.in

† rkapri@iisermohali.ac.in

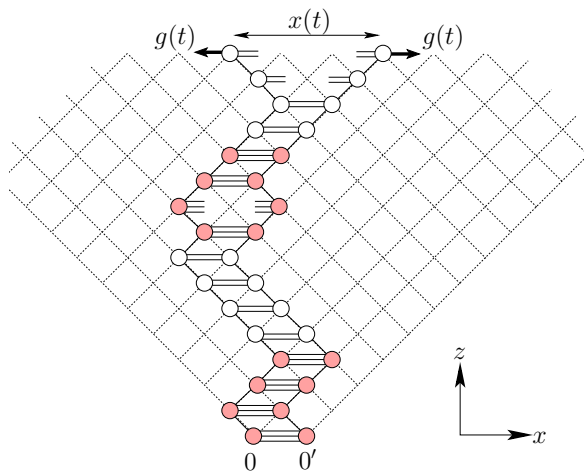


FIG. 1. Schematic diagram of a heterogeneous dsDNA of the type  $(B_4A_4)_2$ , where  $A$  and  $B$  represents base pairs having three and two hydrogen bonds, respectively. One end of the DNA is anchored at the origin ( $O$  and  $O'$ ), and the strands on the free end are subjected to a time-dependent periodic force with frequency  $\omega$  and amplitude  $g_0$ .

DNA are represented by two directed self-avoiding random walks on a  $(d = 1 + 1)$  dimensional square lattice. The walks starting from the origins  $O$  and  $O'$ , which are unit distance apart, are restricted to go towards the positive direction of the diagonal axis ( $z$  direction) without crossing each other. The directional nature of the walks take care of the self-avoidance. Whenever the complementary bases are unit distance apart they gain energy of  $-2\epsilon$  ( $\epsilon > 0$ ) for the base pair of type  $A$  and  $-3\epsilon$  for the base pair of type  $B$ . Here we have assumed that  $\epsilon$  ( $\epsilon > 0$ ), represents the strength of a hydrogen bond.

Two strands of the DNA at one end are always kept fixed at origins  $O$  and  $O'$  and the other end monomers are subjected to a time-dependent periodic force  $g(t)$

$$g(t) = g_0 |\sin(\omega t)|, \quad (1)$$

where  $g_0$  is the amplitude and  $\omega$  is the frequency. The schematic diagram of the model is shown in Fig. 1.

In this paper we consider the following two cases: (i) the base pairs having two hydrogen bonds are anchored at the origins and the time varying force is applied on the base pairs that are bound by three hydrogen bonds, represented by  $(A_n B_n)_M$ , and (ii) the opposite case, i.e., the base pairs having three hydrogen bonds are anchored at the origins and the force is acting on monomers that are bound by two hydrogen bonds (represented by  $(B_n A_n)_M$ ). While the equilibrium results for both the cases are found to be the same, the nonequilibrium results show marked differences.

We perform Monte Carlo simulations of the model using the Metropolis algorithm. The strands of the DNA undergo Rouse dynamics that consists of local corner-flip or end flip moves that do not violate mutual avoidance [25]. The elementary move consists of selecting

a random monomer from a strand, which itself is chosen at random, and flipping it. If move results in the overlapping of two complementary monomers, thus forming a base-pair between the strands, it is always accepted as a move. The opposite move (i.e., unbinding of monomers) is chosen with the Boltzmann probabilities  $\eta = \exp(-2\epsilon/k_B T)$  or  $\eta = \exp(-3\epsilon/k_B T)$  for base pairs of types  $A$  and  $B$ , respectively. If the chosen monomer is unbind, which remains unbind after the move is performed is always accepted. The time is measured in units of Monte Carlo steps (MCSs). One MCS consists of  $2N$  flip attempts, which means that on average, every monomer is given a chance to flip. Throughout the simulation, the detailed balance is always satisfied and the algorithm is ergodic in nature. It is always possible, from any starting DNA configuration, to reach any other configuration by using the above moves. We let the simulation run for  $2000\pi/\omega$  MCSs, so that system reaches the stationary state before taking measurements. Throughout this paper, we have chosen dimensionless quantities. The quantities having dimensions of energy are measured in units of  $\epsilon$  and the quantities that have dimensions of length are measured in terms of the lattice constant  $a$ . In this paper we have taken  $k_B = 1$ ,  $\epsilon = 1$ , and  $a = 1$ .

The separation between the end monomers of the two strands,  $x(t)$ , changes under the influence of the applied external force  $g(t)$ , is monitored as a function of time  $t$ . The time averaging of  $x(t)$  over a complete period

$$Q = \frac{\omega}{\pi} \oint x(t) dt \quad (2)$$

can be used as a dynamical order parameter[26]. From the time series  $x(t)$ , we obtain the extension  $x(g)$  as a function of force  $g$  and average it over 10000 cycles to obtain the average extension  $\langle x(g) \rangle$  as a function of  $g$ . For systems far away from equilibrium, the average extension,  $\langle x(g) \rangle$ , for the forward and backward paths for the periodic force is not the same, and we see a hysteresis loop. The area of hysteresis loop,  $A_{loop}$ , is defined by

$$A_{loop} = \oint \langle x(g) \rangle dg \quad (3)$$

depends upon the frequency  $\omega$  and the amplitude  $g_0$  of the oscillating force. This quantity also serves as another dynamical order parameter.

### III. RESULTS AND DISCUSSIONS

In this section we discuss the results obtained for both the static and the dynamic cases. Let us first take the static case.

#### A. Static Case ( $\omega = 0$ )

In the static case, this model can be solved exactly using the generating function and the exact transfer ma-

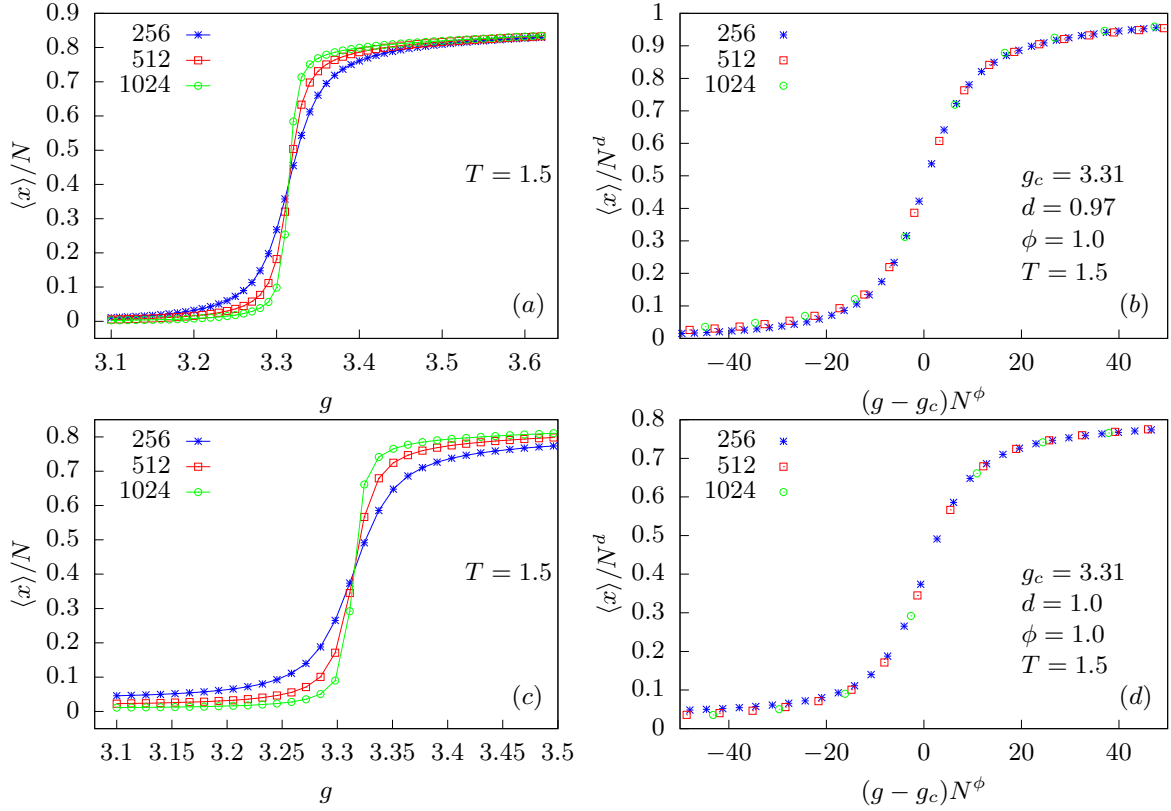


FIG. 2. Scaled extension  $\langle x \rangle / N$ , as a function of constant pulling force  $g$ , obtained using the exact transfer matrix approach, for different chain lengths  $N = 256, 512$ , and  $1024$  at  $T = 1.5$  for (a) the heterogeneous sequence  $(A_{16}B_{16})_M$ . (b)  $\langle x \rangle / N^d$  as a function of  $(g - g_c)N^\phi$  showing a nice collapse of data for  $g_c = 3.31 \pm 0.05$ ,  $d = 0.97 \pm 0.05$ , and  $\phi = 1.0 \pm 0.02$ . (c) For the heterogeneous sequence  $(B_{16}A_{16})_M$ . (d) Collapse of data shown in (c) for  $g_c = 3.31 \pm 0.05$ ,  $d = 1.0 \pm 0.05$ , and  $\phi = 1.0 \pm 0.02$ . The line joining the data points in plots (a) and (c) is just a guide for the eye.

trix techniques. If the partition function of the dsDNA of length  $n$  with separation  $x$  between monomers of the strands is represented by  $\mathcal{D}_n(x)$ , in the fixed distance ensemble, then  $\mathcal{D}_n(x)$  satisfies the recursion relation:

$$\mathcal{D}_{n+1}(x) = [\mathcal{D}_n(x+1) + 2\mathcal{D}_n(x) + \mathcal{D}_n(x-1)] \times \mathcal{C}, \quad (4)$$

where

$$\mathcal{C} = \begin{cases} 1 + (e^{2\beta\epsilon} - 1) \delta_{x,1}, & \text{for base pair type A} \\ 1 + (e^{3\beta\epsilon} - 1) \delta_{x,1}, & \text{for base pair type B.} \end{cases} \quad (5)$$

The above recursion relation can be iterated  $N$  times, with an initial condition  $\mathcal{D}_0(x) = \delta_{x,1}$  to obtain the partition function of the DNA of length  $N$ . The recursion relation (Eq. (4)) with a single base pairing energy (say  $\epsilon$ ) for each base pair such that  $\mathcal{C} = [1 + (e^{\beta\epsilon} - 1) \delta_{x,1}]$  has been solved exactly via the generating function technique [6–8] to obtain the exact unzipping phase diagram. In this method, the singularities of the generating function are calculated. The phase of the DNA is given by the singularity closest to the origin and when the two singularities cross each other a phase transition takes place. Taking the following form for the generating function for

$$\mathcal{D}_n(x),$$

$$\hat{\mathcal{D}}(z, x) = \sum_n z^n \mathcal{D}_n(x) = \kappa^x(z) Y(z), \quad (6)$$

and used in the above recursion relation (Eq.(4) with initial condition  $\mathcal{D}_0(x) = \delta_{x,1}$ ), we obtain  $\kappa(z) = (1 - 2z - \sqrt{1 - 4z})/(2z)$  and  $Y(z) = 1/[1 - z(2 + \kappa(z))e^{\beta\epsilon}]$ . The singularities of  $\kappa(z)$  and  $Y(z)$  are  $1/2$  and  $z_2 = \sqrt{1 - e^{-\beta\epsilon}} - 1 + e^{-\beta\epsilon}$ , respectively. The zero force melting, which comes from  $z_1 = z_2$ , takes place at a temperature  $T_m = \epsilon/\ln(4/3)$ . In the large length limit,  $\mathcal{D}_n(x)$  can be approximated as  $\mathcal{D}_N(x) \approx \kappa^x(z_2)/z_2^{N+1}$ , with the free energy  $\beta F = N \ln z_2 - x \ln \kappa(z_2)$ . The average force required to maintain the separation  $x$ , in a fixed distance ensemble, is then given by

$$g(T) = \frac{\partial F}{\partial x} = -k_B T \ln \kappa(z_2). \quad (7)$$

In the fixed force ensemble, the generating function can be written as

$$\mathcal{G}(z, \beta, g_0) = \sum_x e^{2\beta g_0 x} \sum_n z^n \mathcal{D}_n(x) = \sum_x e^{2\beta g_0 x} \kappa^x(z) Y(z)$$

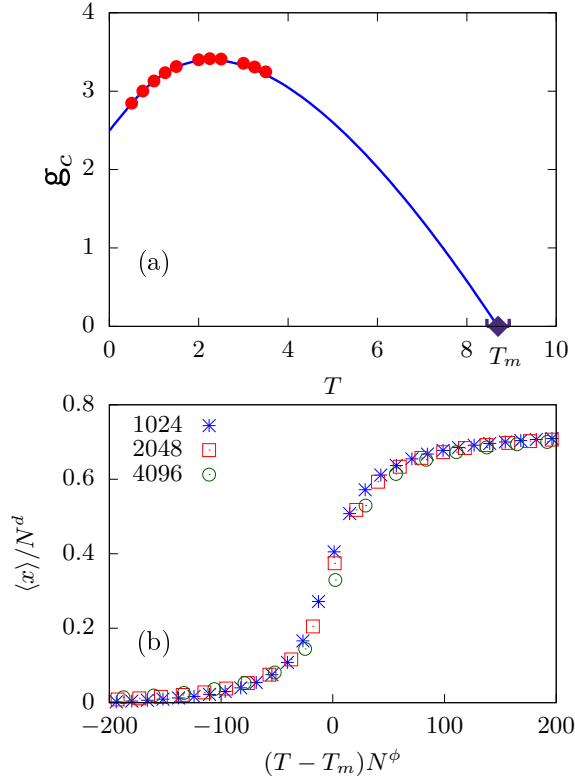


FIG. 3. (a) Critical unzipping force  $g_c$  as a function of temperature  $T$  for the heterogeneous sequence  $(A_{16}B_{16})_M$ . The line is the exact result obtained from the generating function approach [Eq. (9)], and the points are obtained by using finite-size scaling of the force-distance isotherms [Eq. (10)] as obtained from the exact transfer matrix approach. (b) Data collapse of the average distance,  $\langle x \rangle$ , of the heterogeneous sequence  $(A_{16}B_{16})_M$  for  $N = 1024, 2048$ , and  $4096$ . The exponents are  $d = 0.52 \pm 0.02$ ,  $\phi = 0.48 \pm 0.02$  with melting temperature  $T_m = 8.45 \pm 0.25$ .

$$= \frac{Y(z)}{1 - \kappa(z)e^{2\beta g_0}}, \quad (8)$$

which has an additional force-dependent singularity  $z_3 = 1/[2 + 2\cosh(2\beta g_0)]$ . The phase boundary comes from  $z_2 = z_3$ , and is given by

$$g_c(T) = k_B T \cosh^{-1} \left[ \frac{1}{2} \frac{1}{\sqrt{1 - e^{-\beta \varepsilon}} - 1 + e^{-\beta \varepsilon}} - 1 \right], \quad (9)$$

which is same as the phase boundary obtained in the fixed distance ensemble [Eq. (7)]. In the above expression,  $\varepsilon$  is the only free parameter, which can be tuned. For the block copolymer DNA case, in every block, we have  $n$  base pairs each of types  $A$  and  $B$ , giving the total base pairing energy  $(2\varepsilon + 3\varepsilon)n$ . Since the total energy of the block remains the same irrespective of the sequence  $(A_n B_n)_M$  or  $(B_n A_n)_M$ , we seek if an effective base pairing energy  $\varepsilon = 5\varepsilon/2$  in Eq. (9) can give us the exact phase boundary for the block copolymer DNA as obtained by iterating the recursion relation Eq. (4). The

phase diagram of unzipping of a block copolymer DNA (with  $\varepsilon = 5\varepsilon/2$ ) is shown in Fig. 3(a) by solid lines.

The exact transfer matrix technique can be used to obtain many other equilibrium properties which are based on thermal averaging for a finite system size. In this technique, the partition function  $\mathcal{D}_N(x)$  for the DNA of length  $N$ , at any temperature, can be obtained numerically by iterating the above recursion relation [i.e. Eq. (4)]  $N$  times, with an initial condition  $\mathcal{D}_0(1) = 1$ . The equilibrium average separation between the end monomers,  $\langle x \rangle_{\text{eq}}$ , can then be obtained by

$$\langle x \rangle_{\text{eq}} = \frac{\sum_x x \mathcal{D}_N(x) e^{\beta g_0 x}}{\sum_x \mathcal{D}_N(x) e^{\beta g_0 x}}. \quad (10)$$

In Fig. 2, we have plotted the scaled extension  $\langle x \rangle/N$ , as a function of constant pulling force  $g$  for different chain lengths  $N = 256, 512$ , and  $1024$  at  $T = 1.5$  obtained by iterating the recursion relation Eq. (4) for the heterogeneous sequences  $(A_{16}B_{16})_M$  [Fig. 2(a)], in which the base pair of type  $A$  is anchored at the origin and an external force  $g$  is applied on the base pair type  $B$ , and  $(B_{16}A_{16})_M$  [Fig. 2(c)], which is the opposite of the above. From the figure, we can clearly see that the DNA is in the zipped phase at lower  $g$  values and in the unzipped phase when  $g$  exceeds a critical value  $g_c$ . Furthermore, as the length  $N$  of DNA increases, the transition becomes sharper. In the thermodynamic limit, it would become a step function at a critical value  $g_c$ . The point of intersection of these isotherms for various lengths is very close to the critical force  $g_c$ . We use the finite-size scaling, shown in Figs. 2(b) and 2(d), to extract the value of critical force  $g_c$ . The critical force,  $g_c = 3.31 \pm 0.05$  (at  $T = 1.5$ ), is found to be same for the both sequences  $(A_{16}B_{16})_M$  and  $(B_{16}A_{16})_M$  implying that, at equilibrium, it does not matter whether the DNA is unzipped from the end having base pairing with three hydrogen bonds (stronger) or the base pairing with two hydrogen bonds. This is because the unzipping transition is a first-order phase transition. The critical forces obtained at various temperatures using the transfer matrix method are shown in Fig. 3(a) by points. They match exactly with the analytical results given by Eq. (7). The same exact transfer matrix technique could also be used to obtain the melting temperature of the DNA. We again iterate the recursion relations now at zero force value  $g = 0$  and obtain the equilibrium separation between strands at the free end as a function of temperature. We use chain lengths  $N = 1024, 2048$ , and  $4096$ , and the finite-size scaling of the form

$$\langle x \rangle = N^d \mathcal{G}((T - T_m)N^\phi), \quad (11)$$

to obtain the melting temperature  $T_m$ . A nice collapse is obtained for  $d = 0.52 \pm 0.02$ ,  $\phi = 0.48 \pm 0.02$  and  $T_m = 8.45 \pm 0.25$  for sequence  $(A_{16}B_{16})_M$  [shown in Fig. 3(b)]. We have tried various other sequences and found that the melting temperatures for all the heterogeneous sequences allowed in our model are the same.

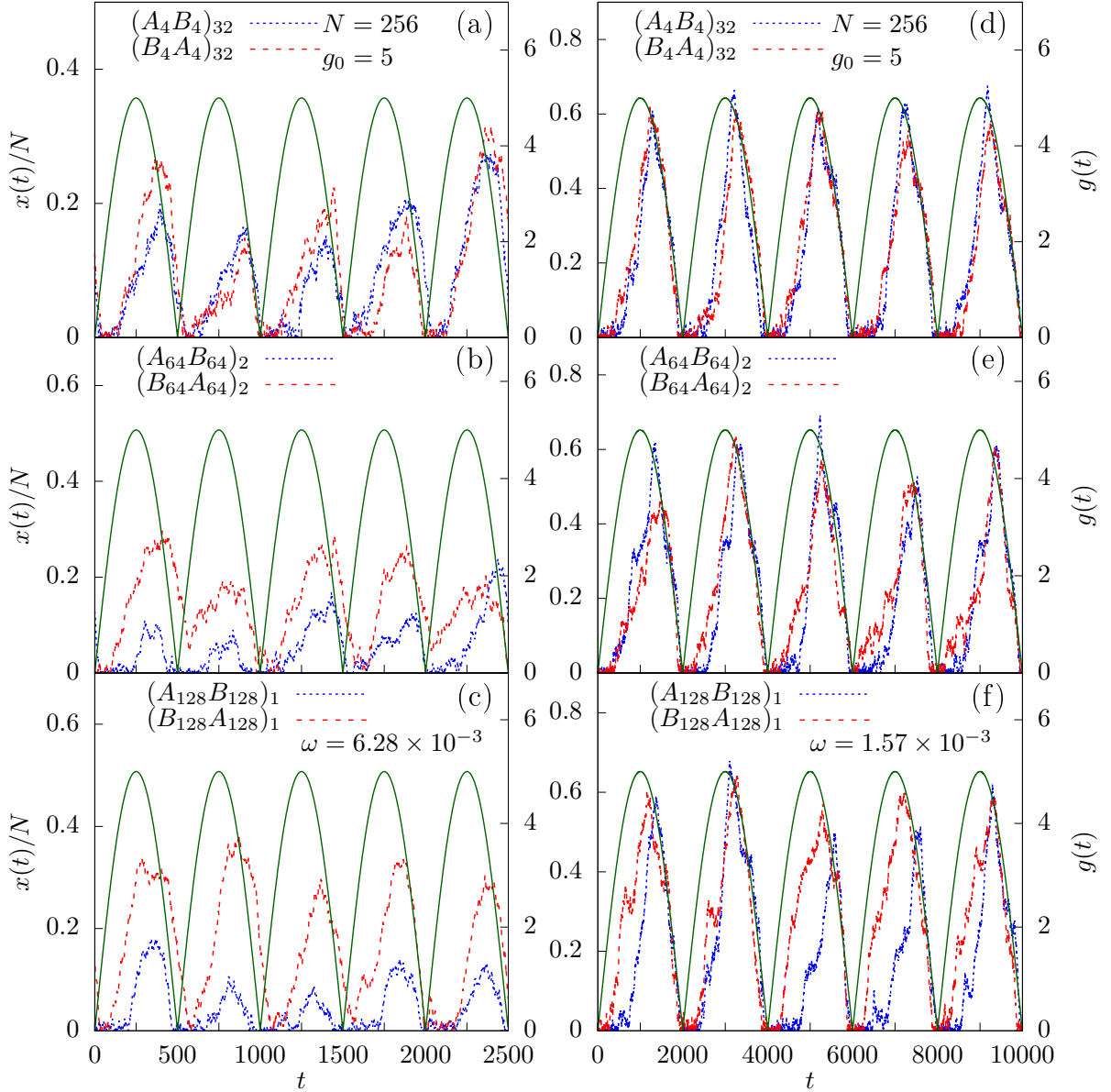


FIG. 4. The extension  $x(t)$  between the end monomers of the two strands of the block copolymer DNA of length  $N = 256$  as a function of time  $t$  when it is subjected to a periodic force of amplitude  $g_0 = 5$  at frequency  $\omega = 6.28 \times 10^{-3}$ . For the sequences (a)  $(A_4B_4)_{32}$  and  $(B_4A_4)_{32}$ , (b)  $(A_{64}B_{64})_2$  and  $(B_{64}A_{64})_2$ , and (c)  $(A_{128}B_{128})_1$  and  $(B_{128}A_{128})_1$ . Plots (d), (e), and (f) are same as plots (a), (b), and (c) at frequency  $\omega = 1.57 \times 10^{-3}$ . The variation of force with time,  $g(t)$ , is represented by solid lines.

The melting temperature obtained by the transfer matrix method is also shown in Fig. 3(a) by a diamond.

### B. Dynamic Case

In the previous section, we have seen that the unzipping of a block copolymer DNA in equilibrium does not depend on whether the force acts on the base pairs of type  $A$  or type  $B$ . However, for the time-dependent periodic force, we find that the unzipping depends on which

base pairs are unzipped first.

In Fig. 4, we have plotted the time variation of external force  $g(t)$  and scaled extension  $x(t)/N$  for the DNA of length  $N = 256$  with respect to time  $t$  for five consecutive cycles when it is subjected to a periodic force of amplitude  $g_0 = 5$  at two different frequencies  $\omega = 6.28 \times 10^{-3}$  and  $1.57 \times 10^{-3}$  at  $T = 4$ . The force increases from zero to a maximum value of  $g_0$ , which is much larger than the critical force  $g_c$  needed to unzip the DNA at equilibrium, and then decreases to zero again. The DNA responds to this external force and starts unzipping slowly. We can

see that there is always a lag between the scaled extension and the force. It is easy to understand that, for a homopolymer DNA, the time required to unzip a dsDNA is directly proportional to its length. The larger the length of the DNA, the more is the unzipping time. However, for a block copolymer DNA, the unzipping time for the DNA of same length can be quite different as it also depends on its sequence. Figure 4(a) shows the time variation of the distance between end monomers of the two strands for sequences of smaller block sizes 8  $[(A_4B_4)_{32}$  and  $(B_4A_4)_{32}]$ . The scaled extension for both sequences is almost the same. However, on increasing the block sizes to 128 but keeping the frequency and amplitude same, the scaled extension for the sequence  $(B_{64}A_{64})_2$  is more than that for the opposite sequence  $(A_{64}B_{64})_2$  [Fig. 4(b)]. On increasing the block size further to 256, the scaled extension for the sequence  $(B_{128}A_{128})_1$  becomes almost double that for the opposite sequence  $(A_{128}B_{128})_1$  as shown in Fig. 4(c). This can be understood as follows. In one cycle of the periodic force with higher frequency ( $\omega = 6.28 \times 10^{-3}$ ), the force changes faster and the system gets less time to relax. Since it is easier to break base pairs with two hydrogen bonds (type A) in comparison with base pairs with three hydrogen bonds (type B), more base pairs are broken for the sequence  $(B_{128}A_{128})_1$  than for the sequence  $(A_{128}B_{128})_1$ , and we see the higher extension. However, on lowering the frequency of the external force to  $1.57 \times 10^{-3}$ , the system gets enough time to relax, and the extension between the strands become almost comparable for both the sequences for all block sizes as shown in Figs. 4(d)-4(f).

### 1. Hysteresis loops

We have seen that the extension  $x(t)$  follows the driving force  $g(t)$  with a lag. When it is averaged over various cycles, we obtain the average extension  $\langle x(g) \rangle$  as a function of force  $g$  showing a closed loop. The shape of a loop tells much about the dynamics of the system and depends on the frequency  $\omega$  and the force amplitude  $g_0$ . For the present problem, the hysteresis loop also depends on the sequence of the block copolymer DNA. In Fig. 5, we have plotted  $\langle x(g) \rangle$  as a function of force  $g$  at four different frequencies  $\omega = 6.28 \times 10^{-3}$ ,  $1.57 \times 10^{-3}$ ,  $3.14 \times 10^{-4}$ , and  $3.49 \times 10^{-5}$  at force amplitude  $g_0 = 5$  for the DNA of length  $N = 256$  with block sizes 8, 128, and 256 at  $T = 4$ . All of them show hysteresis loops but with different shapes. The loops for DNA of smaller block sizes, e.g.,  $(A_4B_4)_{32}$  and  $(B_4A_4)_{32}$  [Figs. 5(a)-5(d)], are almost the same, irrespective of which base pair is acted upon by the driving force. To understand the shapes of the loop, we first note that at higher frequency, i.e.,  $\omega = 6.28 \times 10^{-3}$ , the stationary state of the DNA at  $g = 0$  is a partially unzipped state with an average extension  $\langle x(g) \rangle = 35$ . At this frequency, the force changes very rapidly and the strands of the DNA do not get enough time to relax, and only a small loop is traced by the ex-

tension between them. However, for a relatively lower frequency  $\omega = 1.57 \times 10^{-3}$ , the stationary state of the DNA at  $g = 0$  is a fully zipped configuration with an average extension  $\langle x(0) \rangle = 0$ . The strands now get relatively more time to relax, and the loop area increases. Even at this frequency, the DNA does not get fully unzipped at the maximum force value. This is shown by the rounding of the loop at the maximum force value. The extension increases even though the force decreases. It reaches a maximum for some lower force value, in the backward cycle, and then decreases to zero when  $g = 0$ . On decreasing the frequency further, the isotherms at higher and lower force values start following the same curve for the forward and backward cycles but with a loop in between whose area decreases with decreasing frequency. The situation for the higher block lengths are, however, different. For the sequence  $(A_{128}B_{128})_1$  (third column in Fig. 5), the stationary state at frequency  $\omega = 6.28 \times 10^{-3}$  is a completely zipped configuration with an average extension  $\langle x(g) \rangle \approx 0$  at  $g = 0$  [see Fig. 5(i)]. This is because the driving force is acting on base pairs with three hydrogen bonds having higher strength, and hence only a few base pairs are broken. Therefore the area of the loop traced by the extension between the strands is also small. In contrast, for the sequence  $(B_{128}A_{128})_1$ , the stationary state (at the same frequency) is a partially unzipped DNA. In this case, the driving force can break more bonds as it is acting on the base pairs with two hydrogen bonds and therefore is weaker than the previous case. Therefore, the average extension  $\langle x(g) \rangle$  traces a loop with larger area. On decreasing the frequency to  $\omega = 1.57 \times 10^{-3}$ , the stationary state (at  $g = 0$ ) for the sequence  $(B_{128}A_{128})_1$  changes to a fully zipped configuration [see Fig. 5(j)] as the strands now get enough time to relax and get re-zipped again for forces far below the critical value. On decreasing the frequency further to  $\omega = 3.14 \times 10^{-4}$  [Fig. 5(k)], the strands get equilibrated for smaller and larger force values, and therefore the extension starts following the equilibrium curve at these force values. However, there is still a hysteresis curve at the transition region that decreases on decreasing the frequency of the force. It is found that the size of the hysteresis loop for the sequence  $(B_{128}A_{128})_1$  decreases much faster. The shape of the loop for this sequence starts closing at the center, and the loop divides into two smaller loops and a plateau starts emerging [see Fig. 5(k)]. At frequency  $\omega = 3.49 \times 10^{-5}$ , one of the smaller loop completely disappears, and the other loop is also very small [Fig. 5(l)]. The shape of loop is markedly different for the opposite sequence  $(A_{128}B_{128})_1$  at the same frequency with considerable loop area. For sequences of intermediate block lengths, for example,  $(A_{64}B_{64})_2$  and  $(B_{64}A_{64})_2$  with block length 128 [Figs. 5(e)-5(h)], the hysteresis loops show mixed features as seen for sequences with smaller and larger block lengths (columns one and three of Fig. 5).



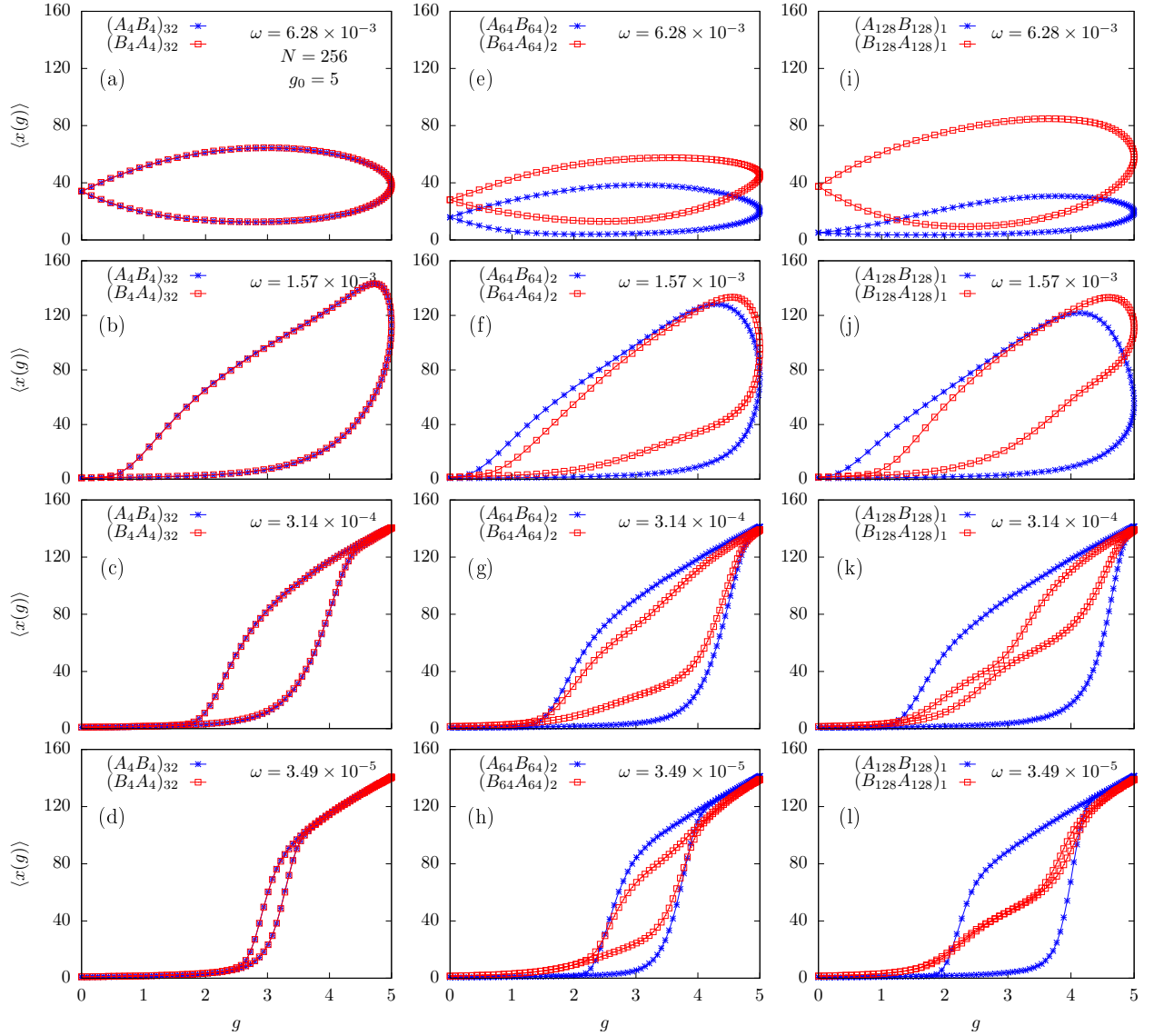


FIG. 5. The force  $g$  vs extension  $\langle x(g) \rangle$  curves averaged over  $10^4$  cycles for the block copolymer DNA of length  $N = 256$  and block sizes 8 (first column), 128 (second column), and 256 (third column) at frequencies  $\omega = 6.28 \times 10^{-3}$  (first row),  $\omega = 1.57 \times 10^{-3}$  (second row),  $\omega = 3.14 \times 10^{-4}$  (third row), and  $\omega = 3.49 \times 10^{-5}$  (fourth row) at force amplitude  $g_0 = 5$  and temperature  $T = 4$ . The data shown in this plot are obtained using Monte Carlo simulations. The line joining the points is just a guide for the eye.

## 2. Loop area

We calculate the area of the hysteresis loops, shown in Fig. 5, numerically using the trapezoidal rule. For the trapezoidal rule to work properly, the intervals should be uniformly spaced. For the problem considered in this paper, the force increases as sine function which gives us non uniformly spaced force values. To convert it into a uniformly spaced interval, we divide the force interval  $g \in [0, g_0]$ , for both the rise and fall of the cycle, into 1000 equal intervals, and then obtain the value of  $\langle x(g) \rangle$  at the end points of these intervals by interpolation using cubic splines of the GNU Scientific Library [27]. The loop

area,  $A_{loop}$ , is then evaluated numerically by using the trapezoidal rule on these intervals.

In Fig. 6, the area of the hysteresis loop,  $A_{loop}$ , is plotted as a function of the frequency,  $\omega$ , of the external pulling force for sequences of various block sizes 8, 128, and 256 of block copolymer DNA of length  $N = 256$  at force amplitude  $g_0 = 5$  and temperature  $T = 4$ . On decreasing the frequency of the pulling force, it is found that the loop area first increases, reaches a maximum value at some frequency  $\omega^*$ , and then decreases with decreasing the frequency further, similar to the hysteresis loop area behavior for a homopolymer DNA under periodic forcing [23]. At a frequency  $\omega^*$ , the natural

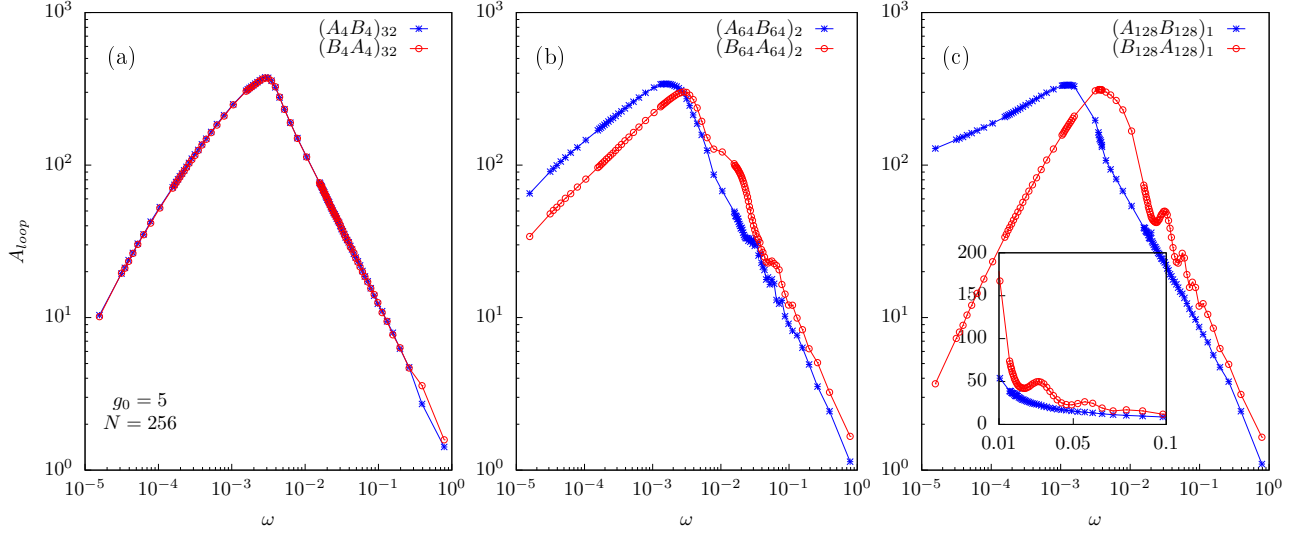


FIG. 6. Area of the hysteresis loop  $A_{loop}$  as a function of frequency  $\omega$  (in log-log scale) at force amplitude  $g_0 = 5$  and length  $N = 256$  for the block copolymer DNA sequences (a)  $(A_4B_4)_{32}$  and  $(B_4A_4)_{32}$ , (b)  $(A_{64}B_{64})_2$  and  $(B_{64}A_{64})_2$ , and (c)  $(A_{128}B_{128})_1$  and  $(B_{128}A_{128})_1$ . The inset shows the higher frequency region (in linear scale), where secondary peaks are visible in  $A_{loop}$  for the sequence  $(B_{128}A_{128})_1$  but are absent for the opposite sequence. In all the plots, the line joining the points is just a guide for the eye.

frequency of the block copolymer DNA matches the frequency of the externally applied force, and we have a resonance with a maximum loop area. For the block copolymer DNA case, the behaviour of  $A_{loop}$  also depends on the DNA sequence used. For sequences of smaller block lengths, e.g.,  $(A_4B_4)_{32}$  and  $(B_4A_4)_{32}$ , the loop area is same, and hence  $\omega^*$  is same for both the sequences [see Fig. 6(a)]. However, this is no longer true for sequences of higher block sizes, where clear differences are seen for the opposite sequences. For example, for block length 256, we can observe that the frequency  $\omega^*$  is higher for the sequence  $(B_{128}A_{128})_1$  than its opposite sequence  $(A_{128}B_{128})_1$  [see Fig. 6(c)]. At frequencies higher than  $\omega^*$ , the former sequence shows secondary peak structures, whereas the sequence  $(A_{128}B_{128})_1$  falls off smoothly without showing any such peaks [see inset of Fig. 6(c)]. On the lower side of frequency  $\omega^*$ , the loop area  $A_{loop}$  falls sharply to zero for the sequence  $(B_{128}A_{128})_1$ , whereas it decreases very slowly for the opposite sequence  $(A_{128}B_{128})_1$ . The secondary peaks in  $A_{loop}$  are the frequencies  $\omega_p = (2p - 1)\pi/2N$ , with  $p = 1, 2, \dots$  as integers, and are higher Rouse modes [23]. These modes are more pronounced for the sequence  $(B_{128}A_{128})_1$ , where the pulling force is applied to  $A$  type base pairs that can be broken at relatively lower force values than  $B$  type base pairs, and hence more base pairs are broken. The two strands thus separated with each other can explore more configurations and can trace a hysteresis loop [See Fig. 5(l)]. This loop has larger area whenever the frequency of the periodic force is  $\omega_p$ , i.e., higher harmonics of the natural frequency of the DNA. In contrast, for the opposite sequence  $(A_{128}B_{128})_1$ , more

force is required to break  $B$  type of base pairs where force is applied, and at higher frequencies only a few base pairs are broken, and the loop traced by unzipped strands is very small and hence no secondary peaks are visible.

We have plotted  $A_{loop}$ , vs  $\omega$  for various sequences at force amplitude  $g_0 = 5$  for block copolymer DNA of three different lengths  $N = 512, 768$ , and  $1024$  in Figs. 7(a) and 7(b). The maximum value of the loop area  $A_{loop}$  is directly proportional to the length of the DNA used in the simulation. Furthermore, the resonance frequency  $\omega^*$ , where  $A_{loop}$  is maximum, decreases with the length of the DNA, suggesting the scaling form

$$A_{loop} = N^d \mathcal{F}(\omega N^z), \quad (12)$$

where  $d$  and  $z$  are exponents, for the loop area  $A_{loop}$ . When  $A_{loop}/N$ , is plotted with the scaled frequency  $\omega N$  (i.e., for exponents  $d = 1$  and  $z = 1$ ), we find a nice data collapse for sequences of all the block sizes [Figs. 7(c) and 7(d)], implying that the loop area for the block copolymer DNA decreases with frequency  $\omega$  as  $A_{loop} \sim 1/\omega$  at higher frequencies (i.e.,  $\omega \rightarrow \infty$ ), similar to the homopolymer case [23].

To obtain the scaling behavior at lower frequencies, we have plotted  $A_{loop}$ , for sequences of various block lengths obtained for a block copolymer DNA of length  $N = 512$ , with respect to  $(g_0 - g_c)^\alpha \omega^\beta$ , at three different force amplitudes  $g_0 = 5.0, 6.5$ , and  $8$  in the low-frequency regime (i.e.,  $\omega \rightarrow 0$ ). In the above expression we have subtracted the critical force  $g_c$  needed to unzip the block copolymer DNA for the static force case [ $g_c(T = 4) = 3.0467$ ]. A similar type of scaling was found earlier for the unzipping of a homopolymer DNA using Brownian dynam-



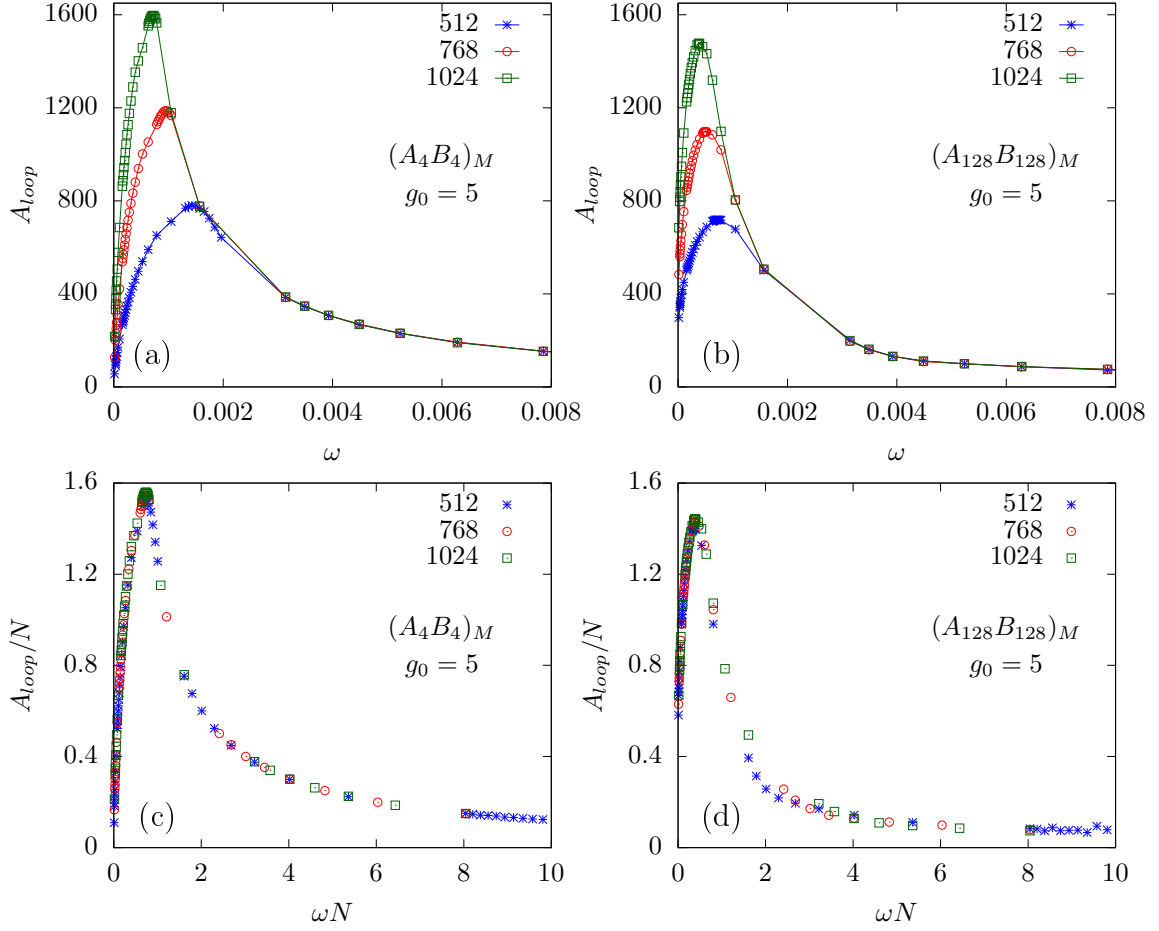


FIG. 7. Area of the hysteresis loop  $A_{loop}$  as a function of frequency  $\omega$  for the block copolymer DNA of lengths  $N = 512, 768, 1024$  at force amplitude  $g_0 = 5$  for sequences (a)  $(A_4B_4)_M$  and (b)  $(A_{128}B_{128})_M$ . Plots (c) and (d) are  $A_{loop}/N$  vs  $\omega N$  for respective sequences in (a) and (b). The line joining the points in these plots is just a guide for the eye.

ics [17, 20] and Monte Carlo simulations [23]. The exponents  $\alpha$  and  $\beta$  are, however, found to be different for these studies. The earlier studies on Brownian dynamics simulations suggested  $\alpha = 1/2$  and  $\beta = 1/2$  [17], which were later modified to  $\alpha = 0.33$  and  $\beta = 1/2$  [20]. On the other hand, the exponents obtained for the Monte Carlo studies were  $\alpha = 1$  and  $\beta = 5/4$  [23]. In Figs. 8(a) and 8(b), we have plotted the scaled data for three sequences  $(A_4B_4)_{64}$ ,  $(A_{64}B_{64})_4$ , and  $(A_{128}B_{128})_2$  and the data for the opposite sequences  $(B_4A_4)_{64}$ ,  $(B_{64}A_{64})_4$ , and  $(B_{128}A_{128})_2$ , respectively. For all these sequences, we obtain a nice collapse for values  $\alpha = 1.0 \pm 0.05$  and  $\beta = 1.25 \pm 0.05$ , the same as the exponents obtained in earlier Monte Carlo studies for the unzipping of a homopolymer DNA by a periodic force [23].

#### IV. CONCLUSIONS

To summarize, in this paper we have studied the unzipping of a block copolymer DNA subjected to a pe-

riodic force with amplitude  $g_0$  and frequency  $\omega$  using Monte Carlo simulations. We obtained results for the static force case and found that the equilibrium results do not depend on the block copolymer DNA sequence and, the temperature-dependent phase boundary  $g_c(T)$ , separating the zipped and the unzipped phases, could be obtained by replacing the binding energy in the exact expression previously obtained for the homopolymer DNA case, by an effective average binding energy per block of the block copolymer DNA sequence. For the dynamic case, the system, however, is not in equilibrium, and results depend on the amplitude and frequency of the periodic force as well as on the DNA sequence. We monitor the separation between the strands of the block copolymer DNA as a function of time at various frequencies and force amplitudes. The averaged separation  $\langle x \rangle$  plotted as a function of force value  $g$  shows a hysteresis loop. The shape of the hysteresis loops is found to be dependent on the frequency of the periodic force and the sequence of block copolymer DNA. For sequences of shorter block lengths, e.g.,  $(A_4B_4)_{32}$  and  $(B_4A_4)_{32}$ , the

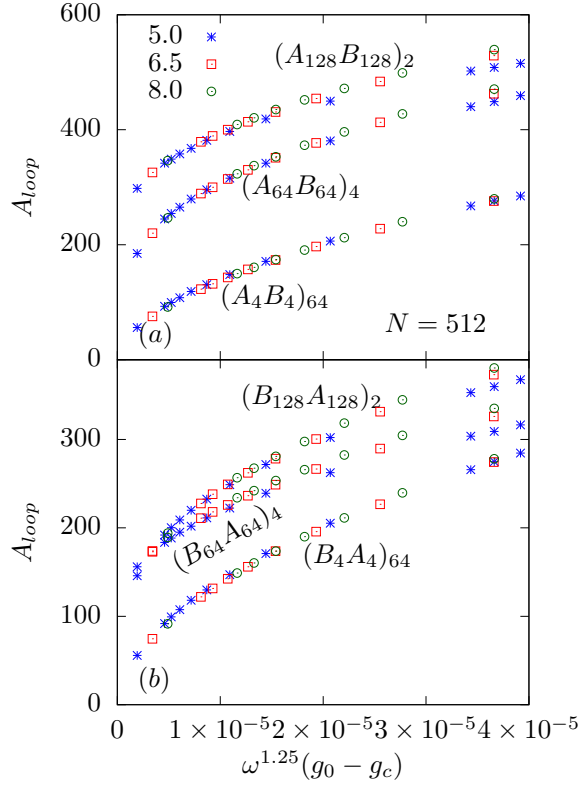


FIG. 8. Scaling of  $A_{loop}$  with respect to  $\omega^{1.25}(g_0 - g_c)$  in the low-frequency regime at force amplitudes  $g_0 = 5.0, 6.5, 8.0$  of a block copolymer DNA of length  $N = 512$  for the sequences (a)  $(A_4B_4)_{64}$ ,  $(A_{64}B_{64})_4$ , and  $(A_{128}B_{128})_2$  and (b)  $(B_4A_4)_{64}$ ,  $(B_{64}A_{64})_4$ , and  $(B_{128}A_{128})_2$ .

loops are found to be the same, with equal area, irrespective of periodic force acting on  $A$ - or  $B$ -type base pairs at all frequencies. However, for longer block lengths, e.g.,  $(A_{128}B_{128})_1$  and  $(B_{128}A_{128})_1$ , the shape of the loops strongly depends on whether the periodic force is applied on  $A$ - or  $B$ -type base pairs. We also obtain the area of the hysteresis loops,  $A_{loop}$  as a function of frequency  $\omega$ . The resonance frequency,  $\omega^*$ , at which the loop area  $A_{loop}$  is maximum is higher for the sequence  $(B_{128}A_{128})_1$ . For frequencies higher than  $\omega^*$ , the loop area for the sequence  $(B_{128}A_{128})_1$  is always more than that for the opposite sequence  $(A_{128}B_{128})_1$ . Another difference is the oscillatory behavior of the  $A_{loop}$  seen for the sequence  $(B_{128}A_{128})_1$ , whereas it is absent for the opposite sequence. For frequencies lower than  $\omega^*$ , we find that the rate at which  $A_{loop}$  decreases with frequency also depends on the block length. The loop area for the sequence  $(B_{128}A_{128})_1$  is found to decrease much faster than the sequence  $(A_{128}B_{128})_1$ . In the lower frequency regime  $A_{loop}$  scales as  $A_{loop} \sim (g_0 - g_c)^\alpha \omega^\beta$  with exponents  $\alpha = 1$  and  $\beta = 5/4$  same as the exponents obtained for periodic forcing of a homopolymer DNA studied earlier [23], whereas in the higher frequencies, the loop area  $A_{loop}$  is found to scale with frequency as  $A_{loop} \sim 1/\omega$  [18, 23]. The differences in exponents observed in Brownian dynamics simulations and the current study requires further investigation and will be the subject of a future study.

## ACKNOWLEDGMENT

We thank S. M. Bhattacharjee, A. Chaudhuri and S. Kalyan for comments and discussions.

- 
- [1] F. Ritort, J. Phys. Condens. Matter **18**, R531 (2006).
  - [2] J. D. Watson, T. A. Baker, S. P. Bell, A. Gann, M. Levine and R. Losick, *Molecular Biology of the Gene*, 5th ed. (Pearson/Benjamin Cummings, Singapore, 2003).
  - [3] S. M. Bhattacharjee, J. Phys. A: Math. Gen **33**, L423 (2000).
  - [4] D. K. Lubensky and D. R. Nelson, Phys. Rev. Lett. **85**, 1572 (2000).
  - [5] K. L. Sebastian, Phys. Rev. E **62**, 1128 (2000).
  - [6] D. Marenduzzo, A. Trovato, and A. Maritan, Phys. Rev. E **64**, 31901 (2001).
  - [7] D. Marenduzzo *et al.*, Phys. Rev. Lett. **88**, 28102 (2002).
  - [8] R. Kapri, S. M. Bhattacharjee, and F. Seno, Phys. Rev. Lett. **93**, 248102 (2004).
  - [9] U. Bockelmann, P. Thomen, B. Essevaz-Roulet, V. Viasnoff, and F. Heslot, Biophys. J. **82**, 1537 (2002).
  - [10] C. Danilowicz, V. W. Coljee, C. Bouzigues, D. K. Lubensky, D. R. Nelson, and M. Prentiss, Proc. Natl. Acad. Sci. U.S.A. **100**, 1694 (2003).
  - [11] C. Danilowicz, Y. Kafri, R. S. Conroy, V. W. Coljee, J. Weeks, and M. Prentiss, Phys. Rev. Lett. **93**, 78101 (2004).
  - [12] K. Hatch, C. Danilowicz, V. Coljee, and M. Prentiss, Phys. Rev. E **75**, 51908 (2007).
  - [13] R. W. Friddle, P. Podsiadlo, A. B. Artyukhin, and A. Noy, J. Phys. Chem. C **112**, 4986 (2008).
  - [14] Z. Tshiprut and M. Urbakh, J. Chem. Phys. **130**, 084703 (2009).
  - [15] P. T. X. Li, C. Bustamante, and I. Tinoco, Proc. Natl. Acad. Sci. U.S.A. **104**, 7039 (2007).
  - [16] A. Yasunaga, Y. Murad, and I. T. S. Li, Phys. Bio. **17**, 011001 (2019).
  - [17] S. Kumar and G. Mishra, Phys. Rev. Lett. **110**, 258102 (2013).
  - [18] G. Mishra, P. Sadhukhan, S. M. Bhattacharjee, and S. Kumar, Phys. Rev. E **87**, 22718 (2013).
  - [19] R. K. Mishra, G. Mishra, D. Giri, and S. Kumar, J. Chem. Phys. **138**, 244905 (2013).
  - [20] S. Kumar, R. Kumar, and W. Janke, Phys. Rev. E **93**, 010402 (2016).
  - [21] T. Pal and S. Kumar, EPL (Europhys. Lett.) **121**, 18001 (2018).
  - [22] R. Kapri, Phys. Rev. E **86**, 41906 (2012).
  - [23] R. Kapri, Phys. Rev. E **90**, 062719 (2014).

- [24] M. S. Kalyan and R. Kapri, J. Chem. Phys. **150**, 224903 (2019).
- [25] M. Doi and S. F. Edwards, *The Theory of Polymer Dynamics* (Oxford University Press, New York, 1986).
- [26] B. K. Chakrabarti and M. Acharyya, Rev. Mod. Phys. **71**, 847 (1999).
- [27] M. Galassi, *Gnu Scientific Library Reference Manual*, 3rd ed. (Network Theory, Bristol, UK, 2009).